

neutrons. The 29.2-keV resonance of Fe would contribute at 325 keV, which coincides with a slight rise in the high-energy wing of resonance No. 13. The 75.6-keV resonance would contribute at 382 keV, which is midway in the low-energy wing of No. 15, and the 85.5-keV resonance contributes at 393 keV, which is in the valley between the first two small peaks above No. 15. The 51-keV resonance of Cr would contribute at 353 keV, which is just below the minimum of No. 10 and might possibly account for the small variation in the cross section at this energy. The 98-keV resonance would contribute at 407 keV, which is in the peak of No. 11. The observed height of No. 11 is 5.7 barns compared with the theoretical height of 5.5 barns. Using the

observed height of 17 barns at the 98-keV resonance and assuming that the neutron beam contains 3% of this low-energy component, the computed cross section for the high-energy neutrons (407 keV) is 5.35 barns, which is only 0.15 barn below the theoretical value.

ACKNOWLEDGMENTS

In conclusion, I wish to express my appreciation to Dr. L. A. Turner for his invaluable help and suggestions, and to Dr. F. E. Throw for his comments and suggestions. I wish also to express my thanks to Dr. R. E. Holland and Dr. F. P. Mooring and to Jack Wallace and the Van de Graaff crew for help with the Van de Graaff electrostatic generator.

Energy Level Spectrum of C^{15} from the Nuclear Reaction $Be^9(Li^7,p)C^{15}\dagger*$

P. G. MURPHY

Enrico Fermi Institute for Nuclear Studies, University of Chicago, Chicago, Illinois

(Received July 8, 1957)

Energy levels of the nucleus C^{15} have been measured by measuring the kinetic energies of proton groups produced in the bombardment of thin beryllium targets with 2-MeV lithium ions, causing the reaction $Be^9(Li^7,p)C^{15}$. The energy levels found were at 0.62, 2.48, 3.08, 4.26, 5.93, 6.58, and 8.18 MeV above the ground state. A continuum of particles was interpreted as due partly to $Be^9(Li^7,pn)C^{14}$. The ground state and the lowest levels were compared with levels in N^{15} ; the presence of the lowest $T=\frac{3}{2}$ level at 11.61 MeV in N^{15} was confirmed. Comparison with the low-lying levels in O^{17} revealed similarity suggested by the analogous shell structures of the two nuclei C^{15} and O^{17} .

INTRODUCTION

EXPERIMENTAL information on the nuclear species C^{15} is scarce for two reasons. In the first place it has a large neutron excess for such a light nucleus, and secondly it has a low binding energy. Possible reactions for producing it are $C^{14}(n,\gamma)C^{15}$, $C^{14}(d,p)C^{15}$, $C^{13}(t,p)C^{15}$, and $Be^9(Li^7,p)C^{15}$.

The first reaction has a Q -value of 1.21 MeV, the second has a Q of -1.007 MeV, and the third has 0.90 MeV; thus none of these is very suitable for the study of excited states of C^{15} . Li^7 , however, also has a low binding energy, giving the last reaction a Q of 9.10 MeV. This allows the production of several excited states with a moderate beam energy.

$C^{14}(n,\gamma)C^{15}$ has been found to have a cross section of less than 10^{-30} cm² for thermal neutrons.¹ $C^{14}(d,p)C^{15}$ has been used to study the ground state of C^{15} .² The

reaction $C^{13}(t,p)C^{15}$ has not been reported. $Be^9(Li^7,p)C^{15}$ has been studied previously in this laboratory.^{3,4}

APPARATUS

(a) Lithium Ion Beam

The production and analysis of the lithium beam have been described in detail previously.^{3,5} A 2-MeV ion beam from a van de Graaff machine fitted with a lithium ion source is passed through a 90°, 36-in. radius electrostatic analyzer, giving a beam of energy 2.00 ± 0.01 MeV. This beam is then analyzed by a $22\frac{1}{2}^\circ$ deflection in a large electromagnet, giving a clear separation of the Li^7 from Li^6 and impurities.

(b) Particle Detecting Cell

The particle detecting apparatus and target chamber are shown in Fig. 1. The lithium ion beam strikes the electrically insulated target and reaction products are collected at 90° to the beam. Their energies can be reduced by insertion of aluminum-foil absorbers and by introduction of gas into the absorption cell. Each

† This research supported in part by the U. S. Atomic Energy Commission.

* Submitted in partial fulfillment of the requirements for the Ph.D. degree at the University of Chicago.

¹ L. Yaffe and W. H. Stevens, *Can. J. Phys.* **29**, 186 (1951); *Phys. Rev.* **79**, 893 (1950).

² Douglas, Broer, Chiba, Herring, and Silverstein, *Phys. Rev.* **104**, 1059 (1956).

³ E. Norbeck, Jr., *Phys. Rev.* **105**, 204 (1957).

⁴ P. G. Murphy, *Bull. Am. Phys. Soc. Ser. II*, **1**, 325 (1956).

⁵ S. K. Allison and C. Littlejohn, *Phys. Rev.* **104**, 959 (1956).

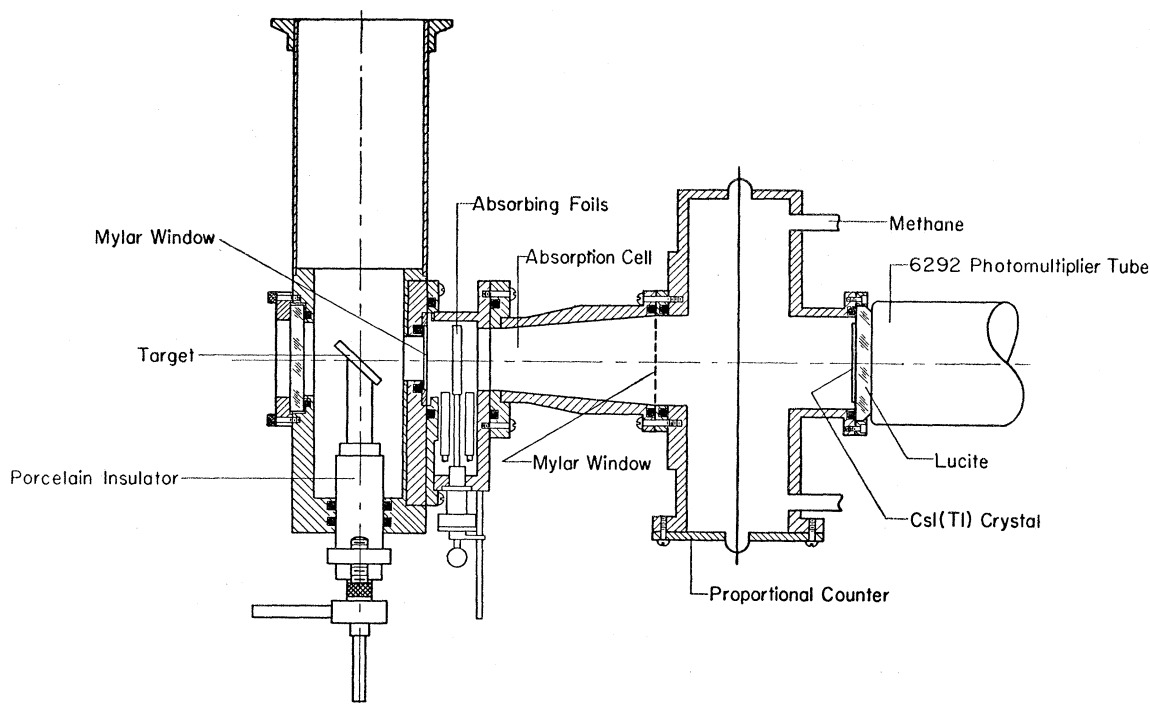


FIG. 1. Target chamber and detector assembly for measuring the energies of proton groups from $\text{Be}^9(\text{Li}^7, p)\text{C}^{16}$ and discriminating against pulses from interfering particles.

foil was carefully weighed. The absorption cell was isolated from the rest of the apparatus by windows of 0.00025-in. Mylar foil.

After passing through the absorbers the particles enter a methane-filled proportional counter. This counter can be used in conjunction with a single-channel pulse-height analyzer either to detect all particles whose production of ions in the counter gas is above a fixed amount or to select only particles whose ion production lies in a chosen interval. Its main purpose in this experiment was to discriminate against β particles from the decay of Li^8 produced in the reaction $\text{Be}^9(\text{Li}^7, \text{Li}^8)\text{Be}^8$, but it was also used to discriminate against tritons and deuterons produced in the reactions $\text{Be}^9(\text{Li}^7, t)\text{C}^{13}$ and $\text{Be}^9(\text{Li}^7, d)\text{C}^{14}$. The counter was operated at 1500 volts with a steady flow of methane at a pressure of 5.6 cm of mercury. The central electrode was of 0.005-in. diameter tungsten wire.

After passing through the absorption cell and the proportional counter the reaction products strike a $1\frac{1}{2}$ mm thick thallium-activated cesium iodide scintillating crystal. The crystal is viewed by a 6292 Dumont photomultiplier tube through a Lucite light-pipe. The crystal was cut with a jeweller's saw from a block and polished with a damp chamois leather. The best resolution was 9% in energy with 9-Mev protons and 8-Mev α particles.

(c) Electronics

A block diagram is shown in Fig. 2. The proportional counter gave a pulse about 200 microseconds long with

a rise time of about 0.1 microsecond. It was shortened in a delay-line pulse shaper delivering a square pulse 4 microseconds long. This was amplified by a Bell-Jordan type amplifier and analyzed in a single-channel pulse-height analyzer.

The cesium iodide pulse traveled through a cathode follower to a Tracerlab nonoverloading linear amplifier. The amplified pulse was then shaped to give a square pulse 7 microseconds long; the shaping circuit also delivered a 1-microsecond gate pulse at a variable instant during the 7-microsecond pulse. A "subtractor" circuit subtracted a chosen voltage from the shaped pulses; this was followed by another stage of amplification (these circuits are accessories of the Tracerlab amplifier). This combination enabled any portion of the spectrum to be spread over the whole range of a Marconi 17-channel pulse-height analyzer.

The gate pulse from the pulse shaper was amplified in a 6BN6 gating tube and added to the signal pulse. The second grid of this tube was controlled by a univibrator which was in turn triggered by the output of the single-channel analyzer. It was thus arranged that a count in the proportional counter corresponding with the desired type of particle would cause the 6BN6 to be cut off so that nothing would be added to the associated cesium iodide pulse. Pulses from the crystal without simultaneous proportional-counter pulses were made into large pulses which would register in the "surplus" channel of the analyzer. The gate pulse was also fed to a point provided on the pulse-height analyzer where it canceled the count in the surplus channel.

EXPERIMENTAL METHOD

The apparatus was calibrated with various groups of protons from the reactions $B^{10}(d,p)B^{11}$, $Be^9(d,p)Be^{10}$, and tritons from the reaction $Be^9(d,t)Be^8$. A 360-kev beam of deuterons from the Institute's Cockcroft-Walton circuit was used. It was also calibrated at this time and during every run with two α -particle groups from a thin source of $ThC+ThC'$. It was found that the drift in amplification was usually imperceptible from day to day; the maximum overnight change was about 1%. Such changes were measured with the α -particle source and allowed for. The system was found to be differentially linear for protons in the range 1–8.5 Mev and for α particles with 3–7 Mev. The pulse height for protons was about twice that for α particles with the same energy. The triton and proton pulse heights were found to be identical at the same energy, contrary to reports from other laboratories.⁶ The energies of the proton and triton groups were taken from Ajzenberg and Lauritsen⁷; the energies of the α particles were taken from Rutherford *et al.*⁸

In the measurements with the lithium beam the proportional-counter single-channel analyzer was usually set to accept all particles which gave a pulse at least as large as that given by a 4.5-Mev proton. For the lowest energy groups of protons there were many interfering groups of tritons and deuterons in the spectrum. In each case the single-channel analyzer was set to select protons in the appropriate part of the spectrum. It was impossible to select only protons over the whole observed spectrum (1–4.5 Mev) because 3-Mev tritons, 2-Mev deuterons, and 1-Mev protons all give the same size pulse in the proportional counter.

The target was beryllium metal evaporated onto nickel; the thicknesses used corresponded with an energy loss of 85 to 135 kev by the 2-Mev lithium beam (40–70 micrograms per square centimeter). For some exploratory measurements a thick target was used.

The total beam charge was measured with an electronic current integrator calibrated with known currents from batteries. The effect of secondary electrons was measured by giving the target a positive bias with batteries.

The background with 2 microamperes of beam was one count per channel per hour. This was never more than 10% of the counting rate at a spectrum peak. The runs varied in length from one to ten hours.

Proton groups were identified by measuring the effect of the aluminum foil absorbers when inserted between the target and the counters. The energy loss for protons was calculated from the data collected by Whaling.⁹

⁶ University of Pittsburgh Technical Report No. VII (unpublished), p. 5.

⁷ F. Ajzenberg and T. Lauritsen, *Revs. Modern Phys.* **27**, 77 (1955).

⁸ Rutherford, Wynn-Williams, Lewis, and Bowden, *Proc. Roy. Soc. (London)* **A139**, 617 (1933).

⁹ R. Fuchs and W. Whaling (private communication).

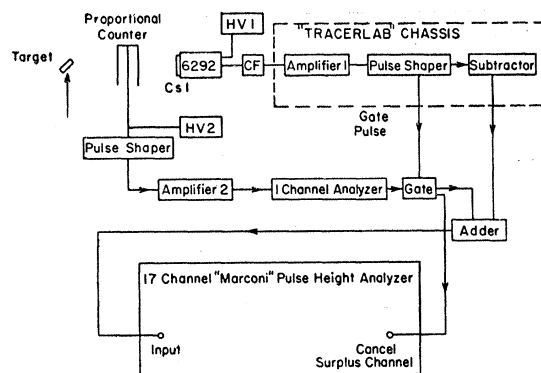


Fig. 2. Block diagram of the electronic circuits used in discriminating against unwanted particles and displaying the pulse heights due to scintillations of the CsI(Tl) detector.

The lowest energy group was not identified in this way but by the fact that to pass this group the setting of the single-channel analyzer was just that necessary to pass deuterons with twice its energy and tritons with three times the energy. Such deuteron and triton groups were produced simultaneously by the reactions $Be^9(Li^7,d)C^{14}$ and $Be^9(Li^7,t)C^{13}$.

RESULTS

The observed spectra consisted of well-defined peaks on a continuous background. The continuum was interpreted as protons and deuterons from the reactions $Be^9(Li^7,pn)C^{14}$ and $Be^9(Li^7,dn)C^{13}$ with Q -values of 7.88 Mev and 0.93 Mev respectively. Two typical spectra are shown in Fig. 3. The results for the peaks identified as protons are shown in Table I. The cross section values are order-of-magnitude estimates; they may be in error by as much as $\pm 50\%$.

The high-energy end of the continuous spectrum is shown in Fig. 4. The lower energy part is uncertain because of the uncertainties involved in the subtraction of the peaks and the impossibility of separating the protons from the deuterons.

The positions of the peaks could be estimated to an accuracy of 100 kev. With the amounts of absorber used a change of 100 kev in the kinetic energy of the emerging protons corresponded with a change of about 40 kev before entering the absorber. Thus the use of absorber improved the energy dispersion. Levels in C^{15} separated by 200 kev could have been resolved.

DISCUSSION OF RESULTS

(a) Isotopic-Spin Multiplets

With the notation $T_3 = \frac{1}{2}$ (number of neutrons – number of protons), C^{15} has $T_3 = +\frac{3}{2}$. The other mass 15 nuclei are N^{15} with $T_3 = +\frac{1}{2}$ and O^{15} with $T_3 = -\frac{1}{2}$. F^{15} , if it existed, would have $T_3 = -\frac{3}{2}$.

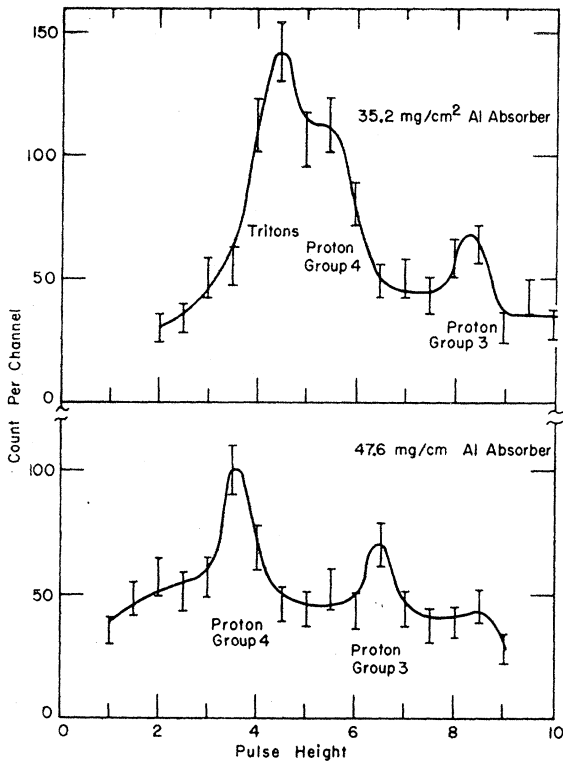


FIG. 3. A typical pulse-height analysis showing two proton groups from $\text{Be}^9(\text{Li}^7, p)\text{C}^{15}$ and a triton group, presumably from $\text{Be}^9(\text{Li}^7, d)\text{C}^{13}$ which has been filtered out by the insertion of additional absorber (lower curve).

(b) Coulomb Corrections

Peaslee¹⁰ has given a quantum-mechanical calculation in which he shows that the difference in Coulomb energy between nuclei with charges Z and $Z+1$ should depend on Z and A according to

$$E(Z+1, Z) = a + b[(Z + \frac{1}{2})/A^{\frac{1}{2}}].$$

The constants a and b may be different for nuclei with $A=4N$, $4N+1$, $4N+2$, and $4N+3$ (N being the number of neutrons).

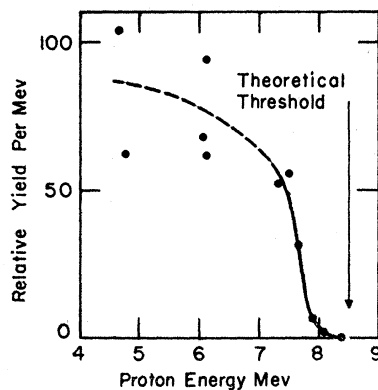


FIG. 4. The upper energy limit of the continuous background, presumably due to protons and deuterons from $\text{Be}^9(\text{Li}^7, pn)\text{C}^{14}$ and $\text{Be}^9(\text{Li}^7, dn)\text{C}^{13}$, on which the monoenergetic proton groups from $\text{Be}^9(\text{Li}^7, p)\text{C}^{15}$ are superimposed.

¹⁰ D. C. Peaslee, Phys. Rev. **95**, 717 (1954).

Kofoed-Hansen¹¹ made a more detailed calculation, finding the expectation value of the operator $\sum_{i>j}(e^2/r_{ij})$, where r_{ij} is the distance between the i th and j th protons. He used simple harmonic oscillator well and square well eigenfunctions for the independent-particle model; he found that well shape had no appreciable effect on the result. His result was that the Coulomb energy correction should have the same form as found by Peaslee, but that the constants a and b should have different values in the different shells.

A plot of the Coulomb correction versus $(Z + \frac{1}{2})/(A^{\frac{1}{2}})$ shows that the actual situation has features of both Peaslee's and Kofoed-Hansen's results (Fig. 5). There is a distinct break between shells and also it appears that the points for $A=4N+3$ lie on one line while the rest lie on another line within one shell. There is only one exception to this for $A < 32$: the mirror pair $\text{O}^{15}-\text{N}^{15}$, for which the correction is known to 5 keV, with $A=4N+3$, lies on the "normal" line. Thus the Coulomb correction to be used when comparing C^{15} with other mass 15 nuclei is not certain. When one uses the

TABLE I. Results.

| C^{15} excitation (Mev) | Proton kinetic energy (Mev) | Q (Mev) | $(\frac{d\sigma}{d\Omega})_{90^\circ}$ (10^{-32} cm ² /sterad) |
|----------------------------------|-----------------------------|-----------------|--|
| 0 | 9.51 ± 0.05 | 9.04 ± 0.05 | 13 |
| 0.62 ± 0.06 | 8.93 | 8.42 | 19 |
| 2.48 ± 0.05 | 7.19 | 6.56 | 6 |
| 3.08 ± 0.04 | 6.64 | 5.96 | 12 |
| 4.26 ± 0.04 | 5.52 | 4.78 | 12 |
| 5.93 ± 0.04 | 3.93 | 3.11 | 15 |
| 6.58 ± 0.04 | 3.34 | 2.46 | 21 |
| 8.16 ± 0.06 | 1.85 | 0.88 | 30 |
| Sum: | | | 1.3×10^{-30} cm ² /sterad |

$A=4N+3$ line, the correction for $\text{C}^{15}-\text{N}^{15}$, including the neutron-proton mass difference, is 2.83 Mev. The "normal" line gives 2.68 Mev. These corrections give excitation energies for the lowest $T=\frac{3}{2}$ state in N^{15} as 11.87 Mev and 11.72 Mev respectively.

(c) Comparison of C^{15} with N^{15}

Excited states of N^{15} have been observed as resonances in the reactions $\text{N}^{14}(n, \alpha)\text{B}^{11}$, $\text{B}^{11}(\alpha, n)\text{N}^{14}$, $\text{C}^{13}(d, p)\text{C}^{14}$, $\text{C}^{14}(p, \gamma)\text{N}^{15}$, $\text{C}^{13}(d, n)\text{N}^{14}$, and $\text{C}^{14}(p, n)\text{N}^{14}$, and as final states in $\text{N}^{14}(d, n)\text{N}^{15}$ and $\text{C}^{14}(d, n)\text{N}^{15}$ (Ajzenberg and Lauritsen).⁷ See Fig. 6.

The only ways that N^{14} can be produced in $T=\frac{3}{2}$ states are by the $\text{C}^{14}+p$ or by $\text{C}^{14}(d, n)\text{N}^{15}$ reactions. The latter has not been taken to high enough energy to produce a $T=\frac{3}{2}$ state. The compound nucleus states in $\text{C}^{14}(p, n)\text{N}^{14}$ must have $T=\frac{1}{2}$ to decay into the ground state of N^{14} , the only state energetically possible in the region of excitation studied. Therefore the only information on $T=\frac{3}{2}$ states in N^{15} comes from a study of

¹¹ O. Kofoed-Hansen, Nuclear Phys. **2**, 441 (1956).

resonances in C¹⁴(*p*, γ)N¹⁵. Such a state should not be a resonance for C¹⁴(*p*,*n*)N¹⁴, which requires a $T=\frac{1}{2}$ state. Since the state is the analog of the ground state of C¹⁵ it would be expected to be well described by the independent-particle model, which is known to give a good description of the low excited states of light nuclei. Such a highly excited independent-particle-model configuration should correspond with a broad state, since it contains one or a few highly excited single-particle states. Such a state has been observed at 11.61 Mev.^{12,13} It has a width of 475 kev. There is a small amount of neutron production from this state, but it is nonreso-

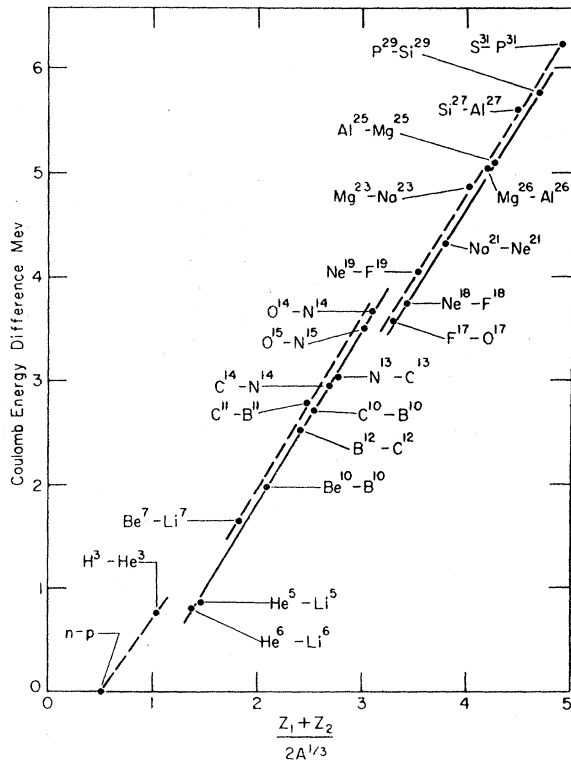


FIG. 5. Coulomb energy differences between isobars with atomic numbers Z and $Z+1$. Breaks in the lines correspond to completion of nuclear shells. The differences for isobars with $A=4N+3$, with the exception of O¹⁵-N¹⁶, lie on (dashed) curves slightly displaced from those for other pairs.

nant, showing that it is contributed by nearby levels. The state has spin $\frac{1}{2}$ and positive parity, so there is no selection rule preventing emission of neutrons other than an isotopic-spin selection rule. Therefore it must be predominantly $T=\frac{3}{2}$, and correspond with the ground state of C¹⁵. This is the highest state observed in reported C¹⁴(*p*, γ)N¹⁵ reactions, so no comparison can be made between higher states of C¹⁵ and N¹⁵.

¹² Bartholomew, Brown, Gove, Litherland, and Paul, Can. J. Phys. 33, 441 (1955).

¹³ Bartholomew, Litherland, Paul, and Gove, Can. J. Phys. 34, 157 (1956).

TABLE II. Comparison of low-lying excited states in the nuclei C¹⁵ and O¹⁷.

| Energy levels in Mev | | Ratio of excitation energies |
|----------------------|-----------------|------------------------------|
| C ¹⁵ | O ¹⁷ | |
| 0.62 | 0.87 | 1.40 |
| 2.48 | 3.07 | 1.24 |
| 3.08 | 3.85 | 1.25 |
| 4.26 | 4.56 | 1.07 |

No $T=\frac{3}{2}$ levels in O¹⁵ have been observed in any reaction.

(d) F¹⁵

Calculation of the Coulomb correction for the pair of isobars C¹⁵ and F¹⁵ shows that F¹⁵ would be unstable to proton emission by 2.3 Mev.

(e) Comparison with O¹⁷

Since C¹⁵ has one neutron outside a closed shell and six protons, it might be expected that the lower part of its level spectrum would be similar to that of O¹⁷, which has one neutron outside a double closed shell. The comparison for the first four levels is shown in Table II. The last column gives the ratio of the excitation energies of corresponding levels. It is seen that there is reasonably close agreement.

(f) Selection Rules in Be⁹(Li⁷,*p*)C¹⁵

It might be expected that there would be some restrictions on the angular momenta and parities of states in C¹⁵ produced in this reaction. The total cross sections for formation of a compound nucleus from the lowest few partial waves of the initial system were calculated from the formula $\sigma_l = (2l+1)\pi\lambda^2 T_l$, where T_l is the penetrability of the Coulomb barrier tabulated by Feshbach, Shapiro, and Weisskopf.¹⁴ The results are given in Table III. It is seen that the $l=1$ cross section is actually larger than the $l=0$ cross section; this is because of the statistical factor $2l+1$ and in spite of the fact that the barrier penetrability decreases from $l=0$ to $l=1$. The $l=2$ and $l=3$ cross sections are also

TABLE III. Theoretical partial-wave capture cross sections in the bombardment of Be⁹ with Li⁷. $\sigma_l = (2l+1)\pi\lambda^2 T_l$, where λ is the wavelength divided by 2π , l is the orbital angular momentum quantum number, and T_l is the penetrability of the Coulomb barrier.

| l | $4/T_l$ | σ_l (cm ²) |
|------|-------------------|----------------------------------|
| 0 | 3.8×10^3 | 1.7×10^{-28} |
| 1 | 6.6×10^3 | 2.9×10^{-28} |
| 2 | 2.6×10^4 | 1.2×10^{-28} |
| 3 | 1.8×10^5 | 0.25×10^{-28} |
| Sum: | | 6.0×10^{-28} |

¹⁴ Feshbach, Shapiro, and Weisskopf, U. S. Atomic Energy Commission Report NYO-3077 (unpublished).

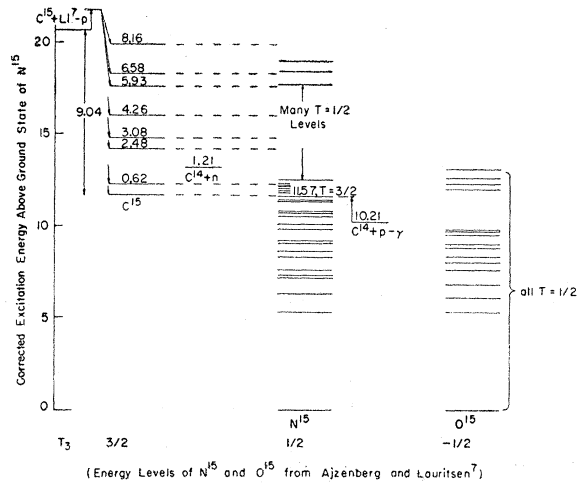


FIG. 6. Energy relations between levels of certain mass 15 isobars, after applying the Coulomb correction and the correction for the n, p mass difference. (The uncorrected experimental energy differences $C^{15}-N^{15}$ and $O^{15}-N^{15}$ are 9.82 and 2.705 Mev respectively.)

comparable. Combined with the fact that the nuclear spins of Li^7 and Be^9 can combine to give resultants of 3, 2, 1, or 0, this makes it apparent that any state with spin $13/2$ and negative parity or spin $11/2$ and positive parity and any state with smaller spin can be produced with comparable intensities. This is due to the large mass of the lithium 7 projectile; it can pass close by the target nucleus and still have a large angular momentum. Comparison of the sum in Table I with that in Table III shows that the total cross section (assuming a uniform angular distribution) for production of C^{15} in any state is about 3% of the theoretical capture cross section. This could be due to competition from the large number of other possible reactions [$Be^9(Li^7, d)C^{14}$, $Be^9(Li^7, t)C^{13}$, $Be^9(Li^7, pn)C^{14}$, $Be^9(Li^7, dn)C^{13}$, $Be^9(Li^7, p2n)C^{13}$, $Be^9(Li^7, tn)C^{12}$, $Be^9(Li^7, \gamma)N^{16}$, $Be^9(Li^7, n)N^{15}$, $Be^9(Li^7, 2n)N^{14}$, $Be^9(Li^7, \alpha)B^{12}$, $Be^9(Li^7, \alpha n)B^{11}$, $Be^9(Li^7, Li^8)Be^8$].

(g) Mass of C^{15}

The $(M-A)$ value for C^{15} in its ground state is 14.35 ± 0.05 Mev from the Q of the ground-state proton group. This agrees with the results of earlier experiments. However, this experiment used thin targets; the earlier experiments used thick targets without any correction being applied. The result also agrees with the more accurate determination by Douglas, Broer, Chiba, Herring, and Silverstein.²

(h) Coulomb Barrier in the Compound Nucleus

The decay of the compound nucleus in this reaction corresponds with the escape of an extra proton from a C^{15} nucleus. If the nuclear radius is given by $r_0 A^{1/3}$, then a value of 1.25×10^{-13} cm for r_0 gives a height of 3.5 Mev for the barrier; 1.5×10^{-13} cm gives 2.0 Mev. In the production of highly excited states of C^{15} the emerging proton has low energy; for high enough excitation the proton has to tunnel through the Coulomb barrier. This should favor the production of those excited states for which the proton can get over the top of the barrier. The production of 1.85-Mev protons, leaving the 8.16-Mev state, was observed to have the highest cross section of all. From this it can be concluded that the barrier is at most 2.0 Mev high and the radius of the highly excited compound nucleus is at least $1.5 \times (16)^{1/3} \times 10^{-13}$ cm. This is in agreement with recent results from high-energy electron scattering and calculations of Coulomb corrections.¹⁵

ACKNOWLEDGMENTS

Thanks are due to John Erwood for running the Kevatron, Caroline Littlejohn for assistance in the early part of the experiment and Sam Iwaoka for maintaining the van de Graaff machine and assisting with the electronics.

I am very grateful to Professor S. K. Allison for valuable encouragement and advice throughout the experiment.

¹⁵ L. Rosenfeld, Nuclear Phys. 2, 450 (1956).